146 (2023) 213283

Contents lists available at ScienceDirect

Biomaterials Advances

journal homepage: www.journals.elsevier.com/materials-science-and-engineering-c

A peptide binding to the tetraspanin CD9 reduces cancer metastasis

Thanawat Suwatthanarak [a,b,c], Kazuma Ito [a], Masayoshi Tanaka [a,d], Kei Sugiura [e], Ayuko Hoshino [e], Yoshitaka Miyamoto [f], Kenji Miyado [f], Mina Okochi [a,*]

[a] Department of Chemical Science and Engineering, Tokyo Institute of Technology, 2-12-1 O-okayama, Meguro-ku, Tokyo 152-8552, Japan
[b] Siriraj Cancer Center, Faculty of Medicine Siriraj Hospital, Mahidol University, 2 Wanglang Road, Bangkok Noi, Bangkok 10700, Thailand
[c] Department of Surgery, Faculty of Medicine Siriraj Hospital, Mahidol University, 2 Wanglang Road, Bangkok Noi, Bangkok 10700, Thailand
[d] Department of Chemical Science and Engineering, Tokyo Institute of Technology, 4259 Nagatsuta-cho, Midori-ku, Yokohama-shi, Kanagawa 226-8501, Japan
[e] School of Life Science and Technology, Tokyo Institute of Technology, 4259 Nagatsuta-cho, Midori-ku, Yokohama-shi, Kanagawa 226-8501, Japan
[f] Department of Reproductive Biology, National Research Institute for Child Health and Development, 2-10-1 Okura, Setagaya-ku, Tokyo 157-8535, Japan

ARTICLE INFO

Keywords:
Peptide
Tetraspanins
CD9
Cancer
Metastasis

ABSTRACT

As an organizer of multi-molecular membrane complexes, the tetraspanin CD9 has been implicated in a number of biological processes, including cancer metastasis, and is a candidate therapeutic target. Here, we evaluated the suppressive effects of an eight-mer CD9-binding peptide (CD9-BP) on cancer cell metastasis and its mechanisms of action. CD9-BP impaired CD9-related functions by adversely affecting the formation of tetraspanin webs—networks composed of CD9 and its partner proteins. The anti-cancer metastasis effect of CD9-BP was evidenced by the *in vitro* inhibition of cancer cell migration and invasion as well as exosome secretion and uptake, which are essential processes during metastasis. Finally, using a mouse model, we showed that CD9-BP reduced lung metastasis *in vivo*. These findings provide insight into the mechanism by which CD9-BP inhibits CD9-dependent functions and highlight its potential application as an alternative therapeutic nano-biomaterial for metastatic cancers.

1. Introduction

Cancer is one of the leading causes of death globally and most cancer deaths are resulted from metastasis—the formation of primary cancer-derived secondary tumors at distant sites [1]. Cancer metastasis is a multi-step process involving a series of events that allow cancer cells to invade from the primary tumor, survive in blood vessels or the lymphatic system, extravasate, and form secondary tumors in distant organs [2]. Due to the complexities of metastasis, clinical approaches against metastatic cancers are limited, which causes poor treatment outcomes and inefficient drug discovery [3]. Thus, the development of strategies and agents to prevent metastatic cancer outgrowth is necessary [3].

The CD9 membrane protein is a member of tetraspanins or the transmembrane 4 superfamily (TM4SF) proteins, defined by similarities in size (approximately 20–30 kDa) and topology (four transmembrane domains together with two extracellular and one intracellular loops) (Scheme 1A) [4]. Through its large extracellular loop (LEL) and four transmembrane regions, CD9 interacts with specific partner proteins, including other tetraspanins, thereby forming tetraspanin webs for partner-dependent functions (Scheme 1A) [4,5]. CD9 is expressed in various cellular components (*e.g.*, the plasma membrane, endocytic compartment, and extracellular vesicles (EV)) and is often concentrated in highly curved membrane subdomains (*e.g.*, microvillar-like projections and filopodia) [6]. Depending on cell types and associated molecules, CD9 plays an important role in many biological and pathological processes, such as motility, fusion, signaling, egg–sperm fusion, virus infection, glomerular disease progression, and cancer metastasis [6–10]. There is abundant evidence suggesting that CD9 has roles in cancer differentiation, migration, invasion, and metastasis because of its specific overexpression in metastatic cancer cell lines, cancer-derived EVs, and late-stage cancers [11–15]. As an organizer of biological membranes, CD9 may induce changes in tetraspanin web organization and/or cancer-specific signaling pathways (*e.g.*, TNF-α and TGF-β) in cancer cells [6,16–18]. During EV-based intercellular communication and metastasis, CD9 in high-curvature regions may be responsible for membrane curvature generation/fusion in EV exocytosis as well as adhesion/fusion in EV endocytosis [4,19,20]. Taken together, the

* Corresponding author at: Department of Chemical Science and Engineering, Tokyo Institute of Technology, 2-12-1-S1-24 O-okayama, Meguro-ku, Tokyo 152-8552, Japan.
E-mail address: okochi.m.aa@m.titech.ac.jp (M. Okochi).

https://doi.org/10.1016/j.bioadv.2023.213283
Received 5 August 2022; Received in revised form 29 November 2022; Accepted 2 January 2023
Available online 6 January 2023

tetraspanin CD9 is a potential therapeutic target for metastatic cancers.

The therapeutic benefit of targeting tetraspanins, nevertheless, is hindered by the adverse impact and inefficient delivery of nucleic acids as well as the issues with antibody size, susceptibility, side effects, and resistance [6,21,22]. Alternatively, peptides or short chains of amino acids with strong binding affinity are characterized by small size, high stability, low cytotoxicity, and possible tunability [22,23]. Hence, peptide utilization may be useful for the therapeutic targeting of tetraspanins, including CD9. We have previously identified an eight-mer CD9-binding peptide (CD9-BP, RSHRLRLH) from the amino-acid sequence of CD9's major partner, EWI-2 protein, by the peptide array technique (Scheme 1B) [24]. CD9-BP showed a good affinity for CD9 *via* self-delivery to the membrane-proximal LEL domain and potentially impaired the partner association of CD9 (Scheme 1B) [24,25]. CD9-BP was earlier used as an optional probe for targeting CD9-enriched nanoscale EVs [24]. Besides, CD9-BP preferentially suppressed the migration of cancer cells rather than normal cells [25]. However, the mechanism by which CD9-BP blocks CD9-related functions and its impact on cancer metastasis is still unknown.

In this study, we first evaluated the effect of CD9-BP on the formation of tetraspanin webs. Furthermore, the abilities of CD9-BP to reduce cancer cell migration and invasion were evaluated. The CD9-BP effects on secretion and uptake of nanoscale EVs or exosomes were also evaluated. Finally, we evaluated the ability of CD9-BP to reduce lung metastasis in a mouse model. The results of these analyses clearly demonstrated that CD9-BP is a promising biomolecule for targeted therapy aimed at preventing metastasis.

2. Results and discussion

2.1. Impact of CD9-BP on tetraspanin web formation of melanoma cells

Tetraspanins recruit and sort partner proteins, including other tetraspanins, and form tetraspanin webs [5,26]. To study the impact of CD9-BP on tetraspanin web formation, helical D-form CD9-BP (Fig. S1) was prepared, labeled, and applied to stain melanoma B16/BL6 cells, which show high CD9 expression and are widely used in studies of cancer metastasis and solid tumor formation [27]. As shown in Fig. 1A, similar stain patterns were observed for fluorescein isothiocyanate (FITC)-labeled CD9-BP and Tide Fluor™ 5WS-labeled CD9 antibody on B16/BL6 cell membranes, supporting the CD9-targeting ability of CD9-BP. Tetraspanin web formation in CD9-BP-treated and untreated cells was next observed by super-resolution stimulated emission depletion (STED) microscopy (Fig. 1B and C). After treatment with CD9-BP at 1000 nM, which previously showed no distinct cytotoxicity [25], we observed that the tetraspanin web diameter of the treated sample was smaller than that of the untreated control (Fig. 1D). Moreover, the number of the observed tetraspanin webs to cell surface area was relatively low in the peptide-treated cells (Fig. S2). These data demonstrated that CD9-BP impaired web formation by CD9 and its partner proteins on B16/BL6 cells. Our data were in agreement with previous estimates of the diameter of tetraspanin webs and were consistent with the previously reported competition of CD9-BP with the interaction between CD9 and its major partner, EWI-2 [25,26,28,29]. Because tetraspanin webs facilitate cell surface protein interactions [30], CD9-BP was expected to have adverse effects on CD9 dynamics and the functions of its partner proteins, particularly in cancer metastasis.

2.2. Impact of CD9-BP on migration and invasion of melanoma cells

Since CD9 is involved in cellular migration and invasion, which are necessary for cancer metastasis [31,32], the effects of CD9-BP on these processes were evaluated. A single cell tracking was conducted to observe the movement of individual untreated and CD9-BP-treated B16/BL6 cells on a culture dish. As shown in Fig. 2A and B, CD9-BP statistically decreased the migration distance of B16/BL6 cells in a dose-dependent manner from 100 nM onwards. Moreover, no adverse effect of CD9-BP on B16/BL6 cell viability was observed at concentrations up to 5000 nM CD9-BP (Fig. S3). In addition to single-cell analyses, the migration of untreated and CD9-BP-treated B16/BL6 cells through a polycarbonate porous membrane was evaluated. The migration percentage was statistically lower for CD9-BP-treated cells than for untreated controls, consistent with the single cell tracking analysis (Fig. 2C). The effect of CD9-BP on the invasion of B16/BL6 cells in collagen type I matrices was also observed. Since the addition of CD9-BP statistically decreased the cancer cell migration at 100 nM (Fig. 2A–C), spheroids of B16/BL6 cells were prepared and embedded in the collagen matrices, which were supplemented with 100 nM CD9-BP. CD9-BP also suppressed the matrix invasion of B16/BL6 spheroids based on the relative change in the spheroid area after 48 h of incubation (Fig. 2D and

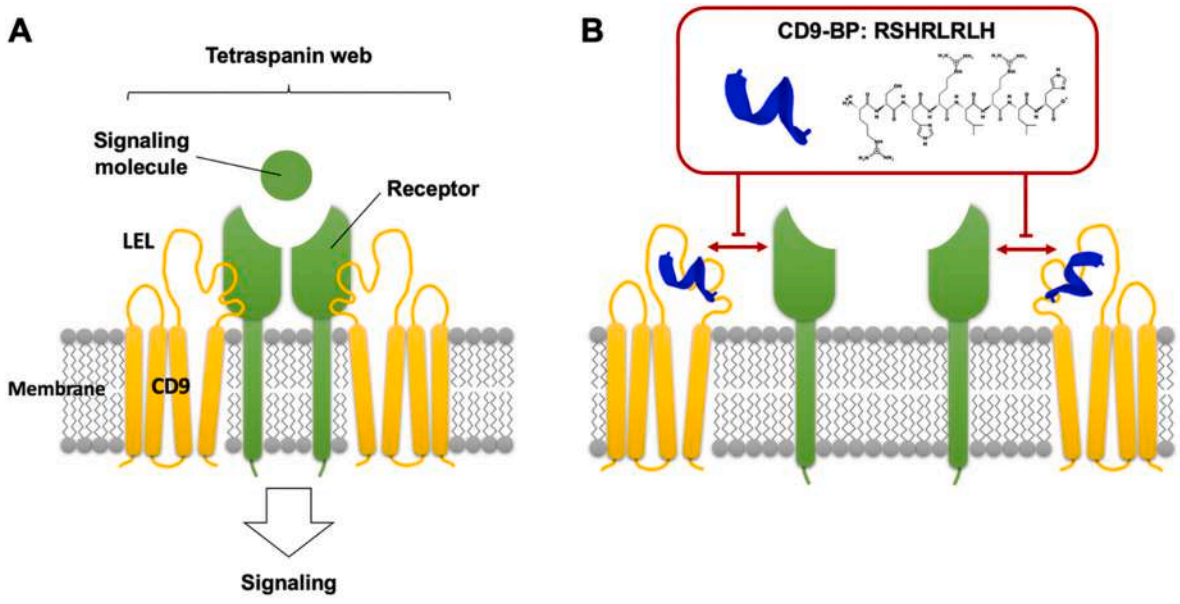

Scheme 1. Schematic illustration of the tetraspanin CD9 and CD9-binding peptide (CD9-BP). A) CD9 associates with signaling partner molecules. B) CD9-BP binds to CD9s large extracellular loop (LEL) and impairs CD9-related functions.

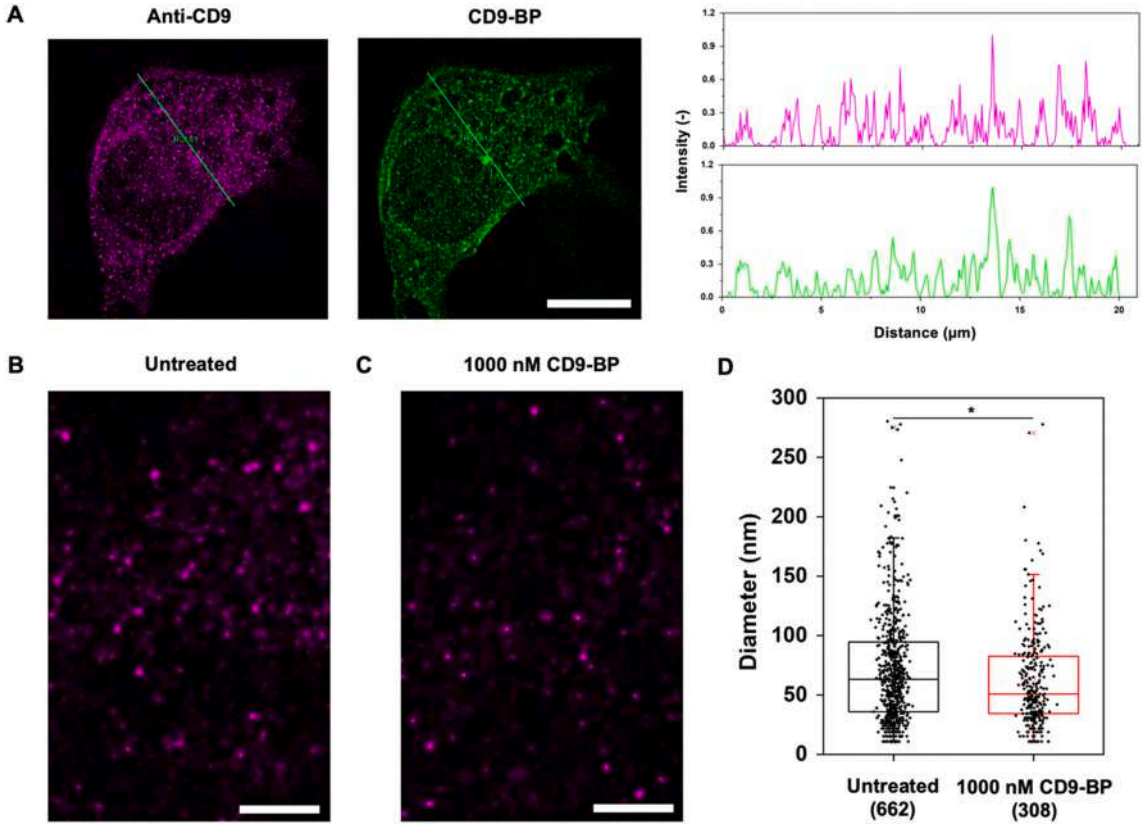

Fig. 1. Impact of CD9-binding peptide (CD9-BP) on CD9 web formation of melanoma cells. A) Fluorescence microscopy images of melanoma B16/BL6 cells co-stained with Tide Fluor™ 5WS-labeled CD9 antibody (pink) and fluorescein isothiocyanate (FITC)-labeled CD9-BP (green). Scale bar, 10 μm. Right graphs show intensity profiles of the labeled CD9 antibody (upper) and the labeled CD9-BP (lower) in a line depicted in the left-hand microscopy images. B) Representative stimulated emission depletion (STED) microscopy image of untreated B16/BL6 cell membranes stained with the labeled CD9 antibody. C) Representative STED microscopy image of CD9-BP-treated B16/BL6 cell membranes stained with the labeled CD9 antibody. Scale bar, 2 μm. D) Box plot of tetraspanin web diameters calculated from intensity profiles in STED microscopy images by the full width at half maximum (FWHM) intensity. The number of the observed webs is indicated in brackets. $*P < 0.01$, Student's *t*-test. (For interpretation of the references to colour in this figure legend, the reader is referred to the web version of this article.)

E). Thus, CD9-BP could decrease both migration and invasion, the initial steps in metastasis, of cancer cells.

2.3. Impact of CD9-BP on cancer cell secretion and uptake of exosomes

Exosomes or nanoscale EVs containing cancer-specific cargoes confer a favorable microenvironment at future metastatic sites and mediate cancer metastasis [33]. CD9 is abundant in high-curvature domains and may be responsible, in part, for membrane curvature, adhesion, and fusion in both exocytic secretion and endocytic uptake of EVs [4,19,20]. A triple-negative human breast cancer cell line (MDA-MB-231), aggressively releasing exosomes [22], was used to examine the effect of CD9-BP treatment on exosome secretion and uptake. MDA-MB-231 cells were cultured using an exosome-free medium with or without CD9-BP, and the cultured medium was then collected to quantify secreted exosomes by a nanoparticle-tracking analysis (NTA) system. As shown in Fig. 3A, CD9-BP reduced the number of secreted exosomes in a concentration-dependent manner. Accordingly, the level of CD63, a well-known exosomal marker [13], in the exosome suspension decreased as the CD9-BP concentration increased (Fig. S4A). Besides, the B16/BL6 and normal human dermal fibroblast (NHDF) cell lines were employed for comparison. As shown in Fig. 3B, treatment with CD9-BP and the CD9 antibody had significant inhibitory effects on exosome secretion in MDA-MB-231 and B16/BL6 cells. Slightly or no inhibitory effect was observed in the normal cell line (NHDF), which secreted fewer exosomes than corresponding estimates for the two highly aggressive cell lines (Fig. 3B). Consistent with the decreased concentration of exosomes, decreased levels of CD63 in the collected exosome suspensions for only MDA-MB-231 and B16/BL6 cells were observed (Fig. S4B). These results suggested that CD9-BP could significantly and negatively affect exosome secretion in highly aggressive cells but not in normal cells.

To study the effect of CD9-BP on exosome uptake, pre-cultured cells were incubated with the same cell-derived and fluorescently-labeled exosomes in a CD9-BP-containing medium. After incubation, the supernatant containing the remaining exosomes was collected and exosome uptake was evaluated based on the decrease in fluorescence intensity. Fig. 3C shows the dose-dependent inhibition of MDA-MB-231 exosome uptake in MDA-MB-231 cells. As shown in Fig. 3D, compared to that of the untreated cells, the exosome uptake abilities of MDA-MB-231 and B16/BL6 cells were inhibited by CD9-BP and CD9 antibody at a concentration of 100 nM, whereas no significant inhibition was observed in NHDF cells. Interestingly, these results were in good agreement with those of a previous study showing that the CD9 antibody could reduce the exosome uptake of B16/BL6 cells by approximately 20 % [19]. The inhibition of uptake was clearly observed in fluorescence images of the MDA-MB-231 and B16/BL6 cells after incubation with fluorescently labeled exosomes (Fig. 3E). In NHDF cells, low exosome uptake was observed with no distinct differences among untreated, CD9-BP-treated, and anti-CD9-treated cells (Fig. 3E). These data demonstrated that CD9-BP could impede exosome uptake in highly aggressive cells but not normal cells. Therefore, CD9-BP has the potential to decrease cancer cell metastasis by inhibiting the secretion and uptake of cancer-derived exosomes.

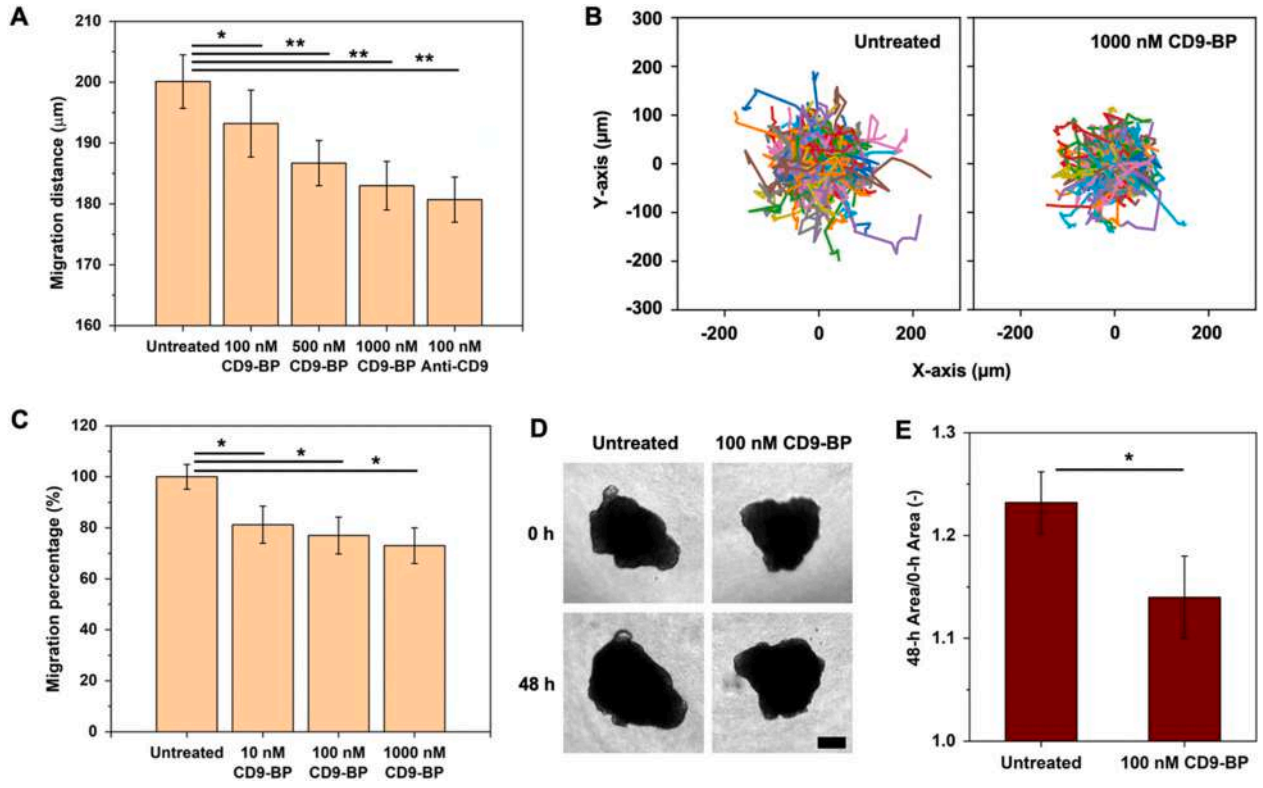

Fig. 2. Impact of CD9-binding peptide (CD9-BP) on the migration and invasion of melanoma cells. A) Migration distance of a single B16/BL6 cell treated with various concentrations of CD9-BP in 12 h. $^{*}P < 0.05$; $^{**}P < 0.01$, Student's *t*-test, n > 100. B) Trajectory plots of B16/BL6 cells untreated (left) and treated with 1000 nM CD9-BP (right) over 12 h. All tracks were set to start at the intersection of x- and y-axes or a common origin. C) Migration percentage of B16/BL6 cells treated with different concentrations of CD9-BP through an 8-μm porous membrane with a Boyden chamber system in 24 h. $^{*}P < 0.05$, Student's *t*-test, n ≥ 3. D) Representative microscopy images of spheroid invasion of B16/BL6 cells untreated and treated with 100 nM CD9-BP in collagen type I matrices (48 h). Scale bar, 200 μm. E) Relative change in the spheroid area in D). Error bars represent standard deviation. $^{*}P < 0.05$, Student's *t*-test, n = 3.

2.4. Impact of CD9-BP on lung metastasis of melanoma cells in vivo

The ability of CD9-BP to prevent metastasis from a primary tumor was finally evaluated in a mouse model [34]. B16/BL6 cells were treated with CD9-BP or control peptide (sequence: AAAA, no CD9-binding ability) and transplanted into C57BL/6 J mice *via* the foot pad (Fig. 4A). After 24 days, the lungs and primary tumors were collected from mice (Fig. 4A). As shown in Fig. 4B and C, B16/BL6 cells treated with CD9-BP resulted in significantly fewer lung nodules or metastases compared with untreated B16/BL6 cells. Furthermore, CD9-BP had a slight effect on the primary tumor weight and length (Figs. 4D and S5). The histological analysis was later performed by sectioning the Bouin's fluid-fixed lungs and primary tumors and staining them with hematoxylin and eosin (H&E) (Fig. 5A and B). The morphology of cancer cells could be abundantly observed in both the lung and primary tumor of the control peptide group (Fig. 5A and B). In contrast, cancer cells were slightly shrunk in the primary tumor, and the number of cancer colonies was reduced in the lung of the CD9-BP group (Fig. 5A and B). These data indicate that CD9-BP could reduce lung metastasis of B16/BL6 cells in a mouse model.

Collectively, we demonstrate that a peptide binding to the tetraspanin CD9 or CD9-BP reduces cancer metastasis. As CD9 is functionally important for the organization of multi-molecular membrane complexes for a wide range of cellular functions, including cancer metastasis, we evaluated the suppressive impacts of CD9-BP on cancer-cell motility and its mechanisms of action to reduce metastasis. Based on the possible architecture of tetraspanin webs reported by Martin et al. [35], we speculate that CD9-BP mainly obstructs the primary extracellular tetraspanin-protein interactions and partially inhibits secondary as well as tertiary heterotetraspanin interactions, causing a decrease in size and number of webs, and an impairment of the related functions (Fig. 6A). In the first step of cancer metastasis, our results suggest that CD9-BP has inhibitory effects on CD9-induced migration and invasion of cancer cells (Fig. 6B). CD9-BP binds competitively to CD9 LEL, serving as the main site for the interactions, including interactions between CD9 and its migration and invasion-mediating partners, such as EWI-2 and integrin beta-1 (Fig. 6B) [36–39]. Moreover, since CD9 may play a key role during the secretion and uptake of cancer-derived exosomes [4,19,20,40], we propose that it impedes the generation of a tumor-favorable microenvironment at metastatic sites by reducing exosome-based cell–cell communication (Fig. 6C). Given the roles of CD9 in membrane dynamics, CD9-BP may decrease CD9-dependent curvature and fusion abilities during the exocytotic exosome secretion or multivesicular body-plasma membrane fusion (Fig. 6C) [4,19,20,41]. Integrin beta-3, an important partner of CD9, has recently been shown to mediate the endocytic exosome uptake of cancer cells; thus, we predicted that CD9-BP can disrupt associations between CD9, integrin beta-3, and other mediators of endocytosis (Fig. 6C) [42]. In addition, CD9-BP may interfere with CD9-related signaling pathways that promote cancer cell metastasis, such as TNF-α and TGF-β [6,16–18,43]. Similar to EWI-2, the parent of CD9-BP, which negatively regulates TGF-β signaling by competitively binding to CD9 in the TβR1-TβR2 association, CD9-BP may weaken the role of CD9 on the association of TβR1 with TβR2 and alter melanoma metastasis [17]. Notably, we herein show that CD9-BP can reduce cancer metastasis *in vivo*, supporting its clinical value. Targeting CD9 by CD9-BP offers the potential to overcome major limitations of typical approaches using antibodies, proteins, and nucleic acids [6,21,22]. Based on its molecular size, CD9 (approximately 4–5 nm on the membrane) may be more accessible by small CD9-BP (approximately 1.08 nm based on 5.4 Å per turn or 3.6 amino acid residues) than

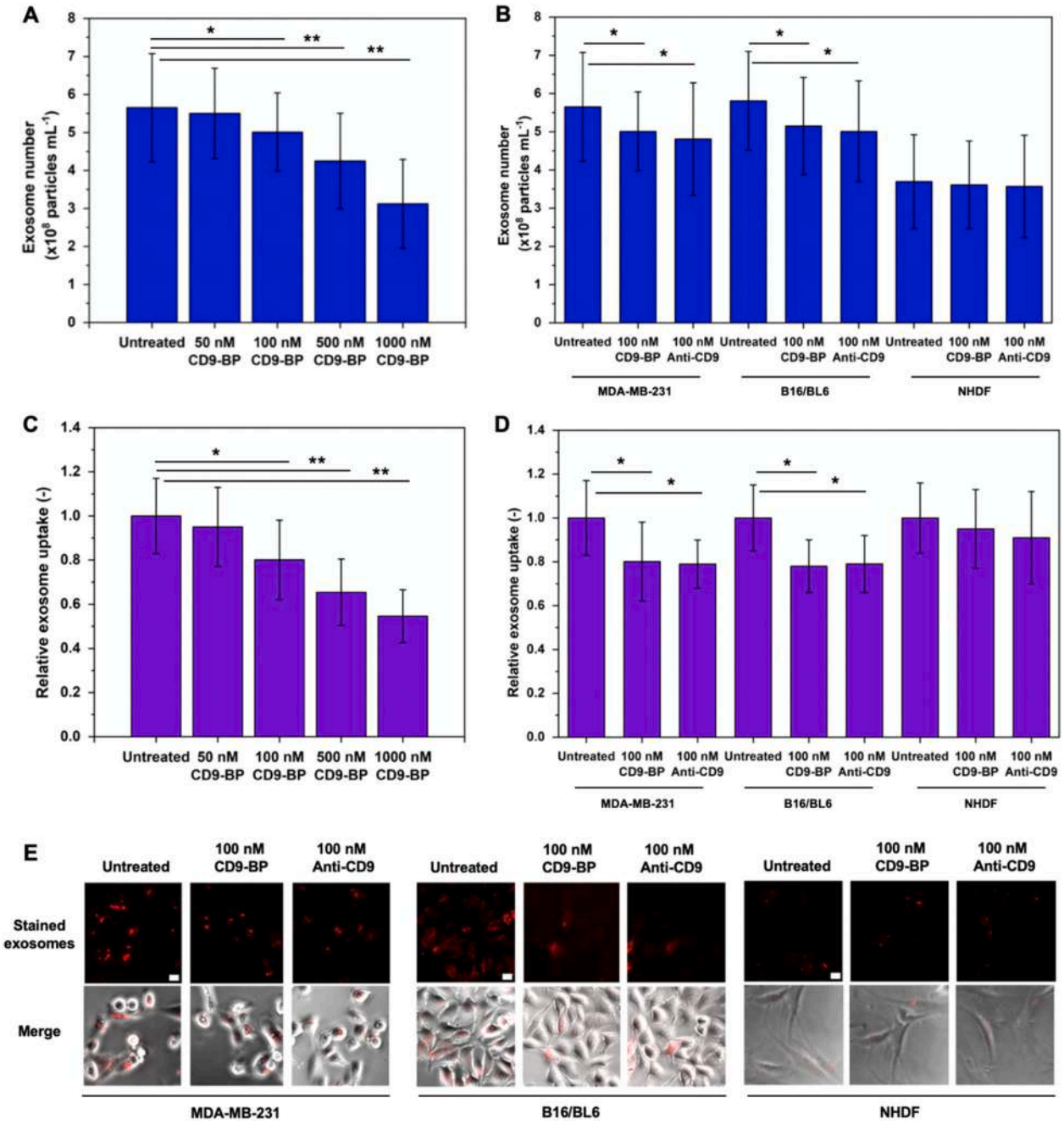

Fig. 3. Impact of CD9-binding peptide (CD9-BP) on cancer cell secretion and uptake of exosomes. A) Number of exosomes secreted from untreated and CD9-BP-treated MDA-MB-231 human breast cancer cells. B) Number of exosomes secreted from untreated, CD9-BP-treated, and anti-CD9-treated MDA-MB-231 and B16/BL6 cells (highly aggressive) as well as normal human dermal fibroblasts (NHDF). C) Exosome uptake ability of untreated and CD9-BP-treated MDA-MB-231 cells. D) Exosome uptake ability of untreated, CD9-BP-treated, and anti-CD9-treated cells for the three representative cell lines. E) Fluorescence microscopy images showing the uptake of stained exosomes in the three representative cell lines. Scale bar, 10 μm. Error bars represent standard deviation. $^{*}P < 0.05$; $^{**}P < 0.01$, paired Student's *t*-test, n = 3.

large CD9-targeting molecules [21]. Compared to other CD9 bio-probes, CD9-BP is more bio-chemically and functionally stable and has relatively low cytotoxicity [44]. Furthermore, CD9-BP prepared by a fully chemical process is highly accessible and feasible for clinical research as well as scale-up commercialization [44]. In the future, the inhibitory mechanisms of CD9-BP's action in cancer metastasis should be further detailed. *In vivo* toxicity studies should also be performed. Potential applications of CD9-BP to other CD9-based pathological activities, such as virus infection and glomerular disease, should be studied [8,9]. Owing to the peptide tunability, the rational optimization and modification of the CD9-BP sequence may yield derivatives with an improved binding affinity [44]. Integrating CD9-BP with other anti-metastatic agents and/or promising drug delivery systems will further enhance the treatment efficiency [44–46]. These findings verify the potential benefits of CD9-BP for metastatic cancer therapy.

3. Conclusion

We demonstrated that CD9-BP is a candidate biomaterial for reducing cancer metastasis. Binding to CD9 LEL, CD9-BP had an adverse effect on the diameter and number of tetraspanin webs—networks of CD9 and its partner proteins. Consequently, CD9-BP decreased cancer

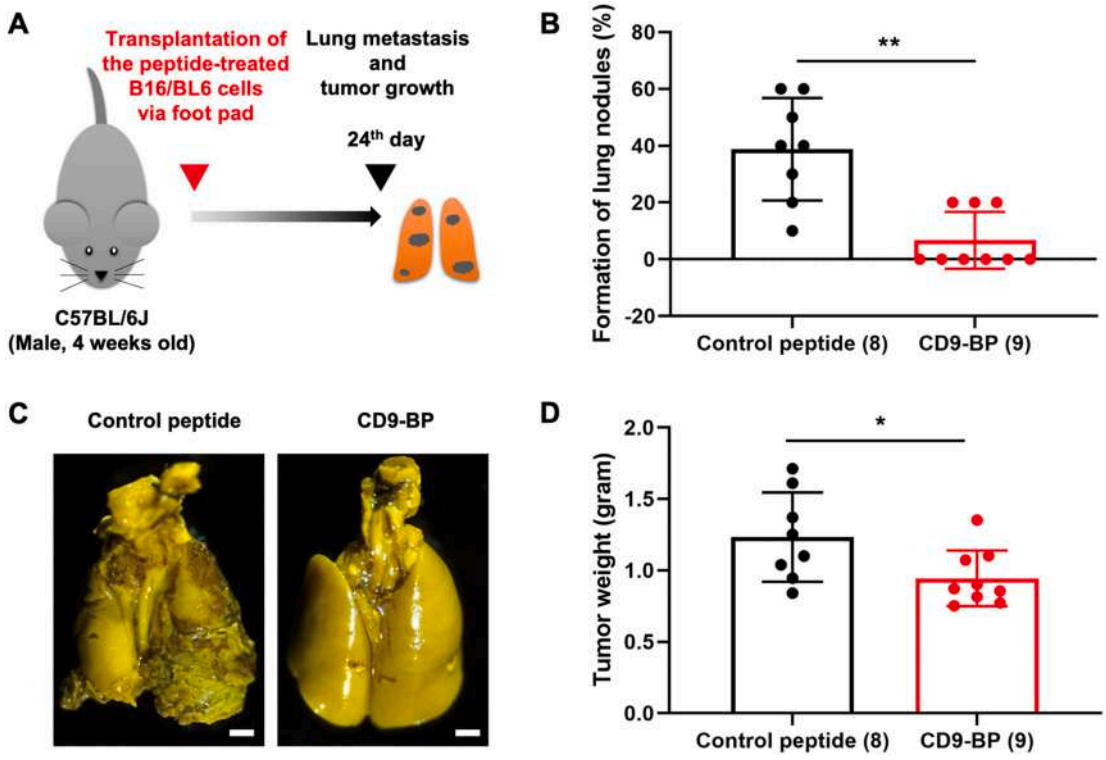

Fig. 4. Impact of CD9-binding peptide (CD9-BP) on the lung metastasis of melanoma cells *in vivo*. A) Experimental schema of the *in vivo* prevention of metastasis from a primary tumor model. B) Percentage formation of the lung nodules. Number in brackets indicates the number of mice. C) Representative images of lungs from mice transplanted with control peptide or CD9-BP-treated B16/BL6 cells. Scale bar, 2 mm. D) Weight of the primary tumors. Error bars represent standard deviations. $^{*}P < 0.05$; $^{**}P < 0.01$, Student's t-test. The control peptide sequence was AAAA.

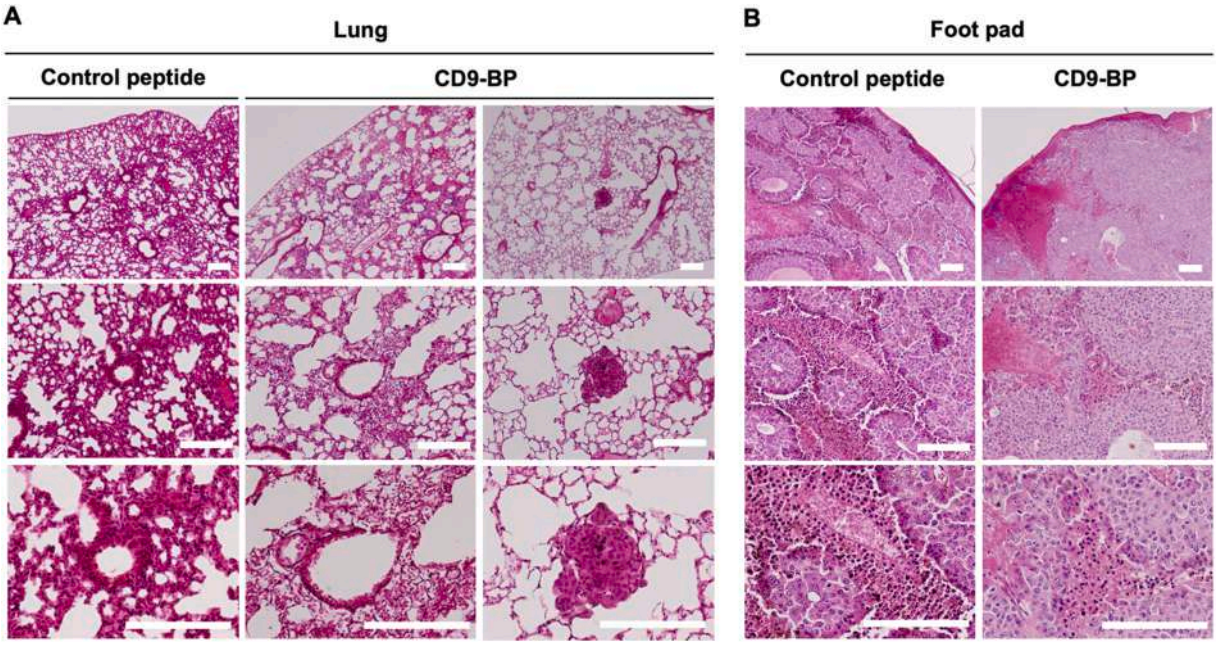

Fig. 5. Hematoxylin and eosin (H&E)-stained images of representative (A) lungs and (B) primary tumors from mice transplanted with control peptide or CD9-binding peptide (CD9-BP)-treated B16/BL6 cells. The image is enlarged from top to bottom. Scale bar, 200 μm.

cell migration and invasion as well as exosome secretion and uptake *in vitro*, all of which are CD9- and metastasis-related processes. CD9-BP also reduced the lung metastasis of melanoma cells in a mouse model. We believe that CD9-BP will be beneficial towards the long-term goal of obtaining effective targeted therapies for metastatic cancers.

4. Materials and methods

4.1. Peptide preparation

D-Form CD9-BP (RSHRLRLH) powder was prepared following

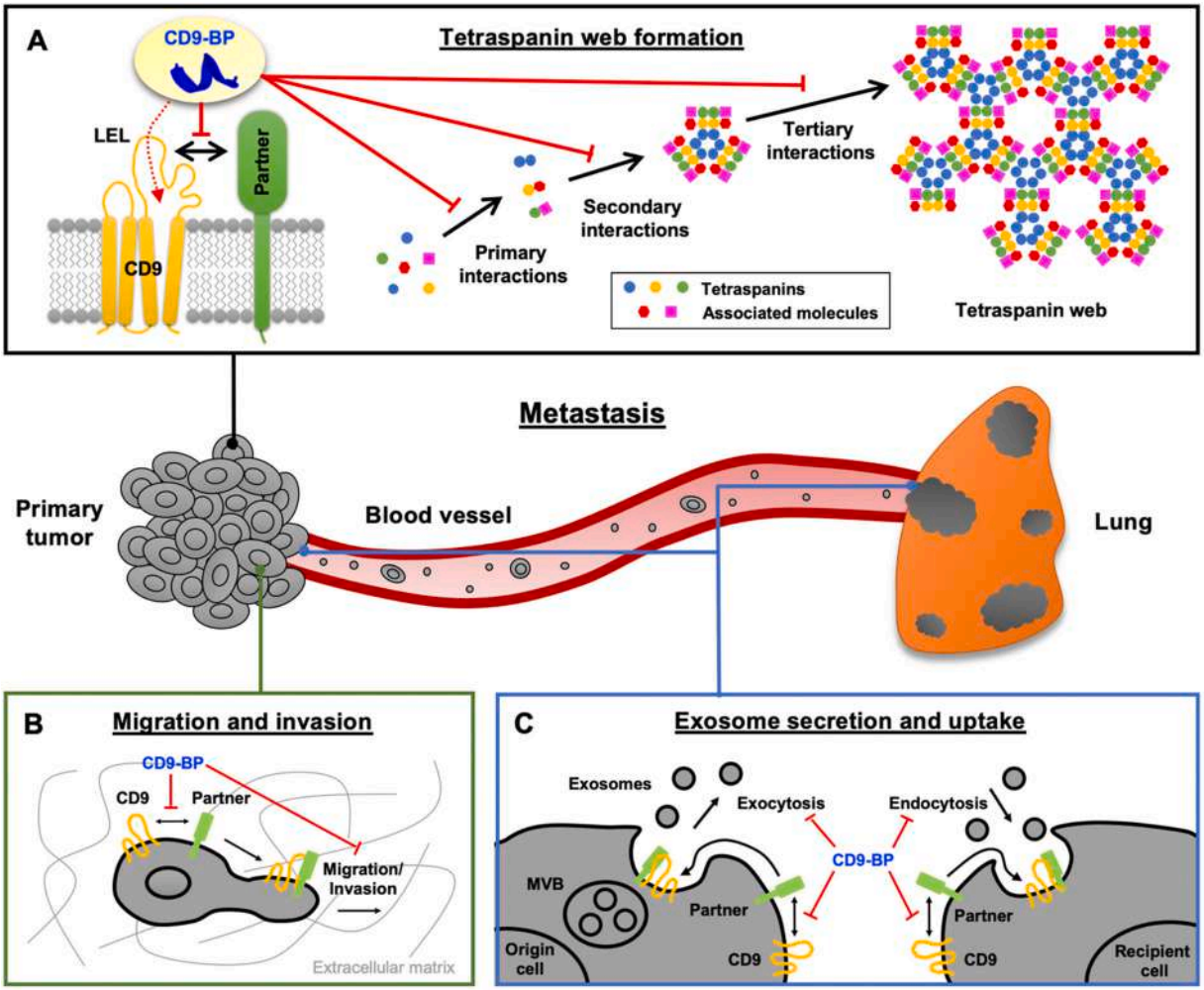

Fig. 6. Overview of the mechanisms by which CD9-binding peptide (CD9-BP) reduces lung metastasis. A) CD9-BP impairs tetraspanin web formation. B) CD9-BP suppresses cell migration and invasion. C) CD9-BP inhibits the secretion and uptake of exosomes.

previously described methods [23,25]. CD9-BP was synthesized on H-Rink-Amide-ChemMatrix® resin using an automated peptide synthesizer (Initiator+; Biotage, Uppsala, Sweden), according to the manufacturer's instructions with some modifications. The synthesis cycle for each amino acid was started with the deprotection of Fmoc group at the N-terminus by 20 % piperidine in *N, N*-dimethylformamide (DMF). DMF was later used to wash the deprotected resin. Next, hydroxybenzotriazole (HOBt), 1-((dimethylamino)(dimethyliminio)methyl)-1H-benzo[d][1,2,3]triazole 3-oxide hexafluorophosphate (HBTU), and *N, N*-diisopropylethylamine (DIEA) were used to activate the carboxyl group of the next Fmoc-amino acid for coupling to the resin N-terminus, followed by DMF washing. After the final elongation, the Fmoc group at the N-terminus was removed by 20 % piperidine in DMF before the resin was washed with DMF and dichloromethane (DCM), respectively. A mixture of trifluoroacetic acid (TFA), 3-methylphenol (*m*-cresol), thioanisole, and ethanedithiol (EDT) (80/2/6/12, v/v/v/v%) was applied to cleave the prepared peptide from the resin and side chain-protecting groups. Chilled diethyl ether was then used to precipitate and wash the peptide. The centrifuged peptide pellet was dissolved in 1 % acetic acid and 30 % acetonitrile in ultra-pure water and finally freeze-dried. High-performance liquid chromatography (HPLC), as well as mass spectrometry (MS) systems, were used to ensure that the target peptide was obtained with a purity of >98 % (Fig. S1).

To label CD9-BP with FITC, the synthesized CD9-BP and FITC 'Isomer I' were mixed with a mole ratio of 1:2 in sodium bicarbonate buffer (pH 8.7) and incubated overnight at room temperature. The FITC-conjugated CD9-BP was purified and confirmed by the HPLC and MS systems.

4.2. Tetraspanin web formation

B16/BL6 melanoma cells (RCB2638; RIKEN BRC, Kyoto, Japan) were cultured in a glass-bottom dish (D11131H; Matsunami, Kishiwada, Japan) using Roswell Park Memorial Institute (RPMI)-1640 medium supplemented with fetal bovine serum (FBS, 10 %), sodium pyruvate (1 mM), and penicillin-streptomycin (100 units mL^{-1}) under 5 % CO_2, 37 °C, and a humidified atmosphere. To prepare cells for staining and imaging, the cells cultured for 24 h were rinsed with phosphate-buffered saline (PBS), fixed with 4 % formaldehyde solution, rinsed with PBS, blocked with 1 % bovine serum albumin (BSA) solution, and rinsed with PBS.

To co-stain the cells with CD9-BP and the CD9-antibody, FITC-labeled CD9-BP was first applied to the prepared cells at a final concentration of 1 μM for 1 h, followed by washing with PBS. Next, Tide Fluor™ 5WS-labeled CD9 antibody (SHI-EXO-M01-TF5; Cosmo Bio, Tokyo, Japan) was incubated with the cells at the final concentration of 50 nM for 1 h before washing with PBS. The co-stained cells were then observed under the THUNDER imaging system (DMi8; Leica, Wetzlar, Germany).

To analyze the impact of CD9-BP on tetraspanin web formation, the cells were cultured with a medium containing 1000 nM CD9-BP overnight before they were prepared as described above. Later, the cells were incubated with the labeled CD9 antibody at the final concentration of

50 nM for 1 h before washing with PBS. Tetraspanin webs on the cells were observed and analyzed using the TCS SP8 STED FALCON microscope system with the pulsed STED 775 nm super-resolution technique (Leica). ImageJ software (National Institutes of Health, Bethesda, MD, USA) was utilized to analyze the number of tetraspanin webs to cell surface area.

4.3. Cancer cell migration and invasion

In the single cell tracking migration assay, B16/BL6 cells were cultured in a 96-well plate under the same conditions described above. After cells reached approximately 15 % confluency, they were stained with CellBrite™ Orange Cytoplasmic Membrane Dye (Biotium, San Francisco, CA, USA), and a new medium containing CD9-BP or CD9 antibody (ab92726; Abcam, Cambridge, UK) was added. The fluorescence microscope with THUNDER live imaging system (Leica) was utilized to track cell movements by obtaining images every 15 min for 12 h. The individual cell movements were analyzed using ImageJ and the Fiji package. The impact of CD9-BP on B16/BL6 cell viability was studied using Cell Counting Kit-8 (Dojindo Molecular Technologies, Inc., Kumamoto, Japan).

In the Boyden chamber assay, B16/BL6 cells in serum-free medium (300 μL, 0.6×10^6 cells mL^{-1}) were seeded in the upper chamber included in the CytoSelect™ 24-Well Cell Migration Assay Kit with an 8 μm-pore size membrane (CBA-101; Cell Biolabs, San Diego, CA, USA). Additionally, 10 % FBS-supplemented medium (500 μL) with or without CD9-BP was placed in the lower well. The cells were allowed to pass through the membrane for 24 h before the migrant cells were harvested, lysed, and stained with the solution of CyQuant GR dye. The fluorescence intensity of the solutions was measured using a microplate reader at 480/520 nm to quantify migrant cells. The assay was strictly conducted following the manufacturer's instructions.

In the invasion assay, B16/BL6 cells (2×10^4 cells mL^{-1}, 100 μL per well) were seeded in a 96-well plate with a round bottom (low attachment, 4870-800LP; IWAKI, Japan) and cultured for 2 days to make cell spheroids. After removing the culture medium, collagen type I-A (Nitta Gelatin, Osaka, Japan) with or without CD9-BP was added to the spheroid and the new medium with or without CD9-BP was placed on the top of the collagen matrix. A microscope was used to obtain images of the spheroids at 0 and 48 h, and ImageJ was applied to analyze the area of spheroids.

4.4. Cancer cell secretion and uptake of exosomes

To evaluate exosome secretion, cells were cultured in 6-cm tissue culture dishes using 5 mL of Dulbecco's modified Eagle medium (DMEM) for MDA-MB-231 and NHDF cell lines (American Type Culture Collection, Manassas, VA, USA), and RPMI-1640 medium for the B16/BL6 cell line. After overnight incubation, the medium was replaced with 5 mL of *exo*-free medium containing CD9-BP or the CD9 antibody, and the cells were further cultured for 72 h. The cultured medium was collected before it was centrifuged in order to remove cell components at 2000 ×*g* for 10 min. To isolate the exosomes, the collected medium was filtered by a 200 nm filter and ultra-centrifuged at 110,000 ×*g* and 4 °C for 80 min. The exosome pellet was washed with PBS (5 mL), ultra-centrifuged, and resuspended with PBS (0.5 mL). The exosome suspension was measured by the NTA system (NanoSight NS300; Malvern Panalytical, Malvern, UK) to count exosomes. The exosome suspension (100 μL) was also applied to quantify CD63 protein using a CD63/CD63 Exosome ELISA kit (HAK-HEL6363–1; Hakarel Inc., Osaka, Japan) according to the manufacturer's instructions.

To evaluate exosome uptake, exosomes from MDA-MB-231, NHDF, or B16/BL6 cells were collected from the cell culture medium by ultracentrifugation, following the methods described above. The exosomes (1.25 μg exosomal protein in 1 mL of PBS) were next labeled with CellBrite™ orange dye (5 μL) for 20 min at 37 °C. The labeled exosomes were pelleted by ultracentrifugation at 110,000 ×*g* and 4 °C for 80 min to remove the excess dye in the supernatant. The labeled exosomes were washed with PBS (1 mL) and again pelleted by ultracentrifugation. The labeled exosomes were re-suspended in the culture medium (1 mL, 1.25 μg of exosomal protein) containing CD9-BP or the CD9-antibody. The exosome suspension prepared from each cell line (100 μL, 0.125 μg of exosomal protein) was immediately added to the pre-cultured MDA-MB-231, NHDF, or B16/BL6 cells in a 96-well plate, followed by overnight incubation. The supernatant containing the remained exosomes was collected and fluorescence was measured using a microplate reader to evaluate exosome uptake based on the decrease in fluorescence intensity. Exosome uptake was also observed under a fluorescence microscope.

4.5. Lung metastasis in vivo

B16/BL6 cells were cultured in three 10 cm dishes, trypsinized, and collected by centrifugation. The cells were next suspended in 2 mL of serum-free DMEM before 800 μL of the cell suspension was mixed with CD9-BP or control peptide (sequence: AAAA) solution (80 μL, 1 mM). The cell-peptide mixture was incubated for 1 h at room temperature before transplantation (3×10^5 cells, 30 μL) into the foot pad of a mouse (C57BL/6 J, male, 4 weeks old, purchased from Japan SLC Inc., Shizuoka, Japan). There was no administration of the peptide after the transplantation. As soon as the first mouse died, the remaining mice were euthanized on day 24 after the transplantation. The chest was next exposed, followed by injection with Bouin's fixative solution (FUJIFILM Wako Pure Chemical Corp., Osaka, Japan) to the upper part of the trachea using a syringe to expand the lungs. Then, the lungs were detached from the body and transferred to Bouin's fixative solution in a 50 mL tube. Furthermore, the primary tumor at the foot pad was excised and transferred to Bouin's fixative solution. The weight of the primary tumor was measured by subtracting the weight of hindlimb with the implanted cells by the weight of hindlimb without the implanted cells. For the histological analysis, the Bouin's fluid-fixed lungs and primary tumors were sectioned, stained with H&E, and finally observed under a microscope with digital camera. The animal experiments were approved by the animal ethics committee of the National Research Institute for Child Health and Development of Japan, and conducted in accordance with the relevant guidelines for the care and use of laboratory animals (experimental number: 04–004).

4.6. Statistical analysis

All experimental data are presented as mean ± standard deviation of at least three samples. The difference was evaluated using the Student's *t*-test.

CRediT authorship contribution statement

Conceptualization, T.S., K.M. and M.O.; Methodology, T.S., K.I., M. T., Y.M., K.M. and M.O.; Validation, M.T., A.H., Y.M., K.M. and M.O.; Formal analysis, T.S., M.T., Y.M., K.M. and M.O.; Investigation, T.S., K.I., K.S., Y.M. and K.M.; Resources, A.H., K.M. and M.O.; Data curation, T.S., K.M. and M.O.; Writing—original draft preparation, T.S. and K.I.; Writing—review and editing, M.T., A.H., Y.M., K.M. and M.O.; Visualization, T.S. and K.I.; Supervision, A.H., K.M. and M.O.; Project administration, M.O.; Funding acquisition, M.T., A.H., Y.M., K.M. and M.O. All authors have approved the published version of the manuscript.

Declaration of competing interest

The authors declare that they have no known competing financial interests or personal relationships that could have appeared to influence the work reported in this paper.

Availability of data and materials

The figures that support the findings of this study are available in the online supplementary data. The rest of the data are also available from the corresponding author upon request.

Acknowledgements

We highly appreciate Mr. Takeshi Chiaki, Ms. Hiroko Kato and Mr. Takeshi Igarashi at Leica (Tokyo, Japan) for supporting the STED observation. The present study was funded by the Grants-in-Aid for Scientific Research from the Ministry of Education, Culture, Sports, Science and Technology of Japan (21H01726, 21H01725, 22K19913). Partially, this work was supported by the Moonshot Research and Development Program from the Japan Agency for Medical Research and Development (AMED) (JP21zf0127004), and the Cross-ministerial Strategic Innovation Promotion Program (SIP) for "Intelligent Processing Infrastructure of Cyber and Physical Systems" from the New Energy and Industrial Technology Development Organization (NEDO) of Japan.

Appendix A. Supplementary data

Supplementary figures to this article can be found online at https://doi.org/10.1016/j.bioadv.2023.213283.

References

[1] H. Dillekås, M.S. Rogers, O. Straume, Are 90% of deaths from cancer caused by metastases? Cancer Med. 8 (2019) 5574.
[2] J. Fares, M.Y. Fares, H.H. Khachfe, H.A. Salhab, Y. Fares, Molecular principles of metastasis: a hallmark of cancer revisited, Signal Transduct. Target. Ther. 5 (2020) 28.
[3] R.L. Anderson, T. Balasas, J. Callaghan, R.C. Coombes, J. Evans, J.A. Hall, S. Kinrade, D. Jones, P.S. Jones, R. Jones, J.F. Marshall, M.B. Panico, J.A. Shaw, P. S. Steeg, M. Sullivan, W. Tong, A.D. Westwell, J.W.A. Ritchie, A framework for the development of effective anti-metastatic agents, Nat. Rev. Clin. Oncol. 16 (2019) 185.
[4] R. Umeda, Y. Satouh, M. Takemoto, Y. Nakada-Nakura, K. Liu, T. Yokoyama, M. Shirouzu, S. Iwata, N. Nomura, K. Sato, M. Ikawa, T. Nishizawa, O. Nureki, Structural insights into tetraspanin CD9 function, Nat. Commun. 11 (2020) 1606.
[5] M.E. Hemler, Tetraspanin functions and associated microdomains, Nat. Rev. Mol. Cell Biol. 6 (2005) 801.
[6] A. Lorico, M. Lorico-Rappa, J. Karbanová, D. Corbeil, G. Pizzorno, CD9, a tetraspanin target for cancer therapy? Exp. Biol. Med. 246 (2021) 1121 (Maywood).
[7] K. Miyado, G. Yamada, S. Yamada, H. Hasuwa, Y. Nakamura, F. Ryu, K. Suzuki, K. Kosai, K. Inoue, A. Ogura, M. Okabe, E. Mekada, Requirement of CD9 on the egg plasma membrane for fertilization, Science 287 (2000) 321.
[8] J.T. Earnest, M.P. Hantak, K. Li, P.B. McCray, S. Perlman, T. Gallagher, The tetraspanin CD9 facilitates MERS-coronavirus entry by scaffolding host cell receptors and proteases, PLoS Pathog. 13 (2017), e1006546.
[9] H. Lazareth, C. Henique, O. Lenoir, V.G. Puelles, M. Flamant, G. Bollée, C. Fligny, M. Camus, L. Guyonnet, C. Millien, F. Gaillard, A. Chipont, B. Robin, S. Fabrega, N. Dhaun, E. Camerer, O. Kretz, F. Grahammer, F. Braun, T.B. Huber, D. Nochy, C. Mandet, P. Bruneval, L. Mesnard, E. Thervet, A. Karras, F.L. Naour, E. Rubinstein, C. Boucheix, A. Alexandrou, M.J. Moeller, C. Bouzigues, P. L. Tharaux, The tetraspanin CD9 controls migration and proliferation of parietal epithelial cells and glomerular disease progression, Nat. Commun. 10 (2019) 3303.
[10] F. Vences-Catalán, S. Levy, Immune targeting of tetraspanins involved in cell invasion and metastasis, Front. Immunol. 9 (2018) 1277.
[11] M. Hemler, Tetraspanin proteins promote multiple cancer stages, Nat. Rev. Cancer 14 (2014) 49.
[12] P. Kischel, A. Bellahcene, B. Deux, V. Lamour, R. Dobson, E. DE Pauw, P. Clezardin, V. Castronovo, Overexpression of CD9 in human breast cancer cells promotes the development of bone metastases, Anticancer Res. 32 (2012) 5211.
[13] Y. Yoshioka, Y. Konishi, N. Kosaka, T. Katsuda, T. Kato, T. Ochiya, Comparative marker analysis of extracellular vesicles in different human cancer types, J. Extracell. Vesicles 2 (2013) 20424.
[14] A. Hoshino, H.S. Kim, L. Bojmar, K.E. Gyan, M. Cioffi, J. Hernandez, C. P. Zambirinis, G. Rodrigues, H. Molina, S. Heissel, M.T. Mark, L. Steiner, A. Benito-Martin, S. Lucotti, A.Di Giannatale, K. Offer, M. Nakajima, C. Williams, L. Nogués, F.A.Pelissier Vatter, A. Hashimoto, A.E. Davies, D. Freitas, C.M. Kenific, Y. Ararso, W. Buehring, P. Lauritzen, Y. Ogitani, K. Sugiura, N. Takahashi, M. Alečković, K. A. Bailey, J.S. Jolissant, H. Wang, A. Harris, L.M. Schaeffer, G. García-Santos, Z. Posner, V.P. Balachandran, Y. Khakoo, G.P. Raju, A. Scherz, I. Sagi, R. Scherz-Shouval, Y. Yarden, M. Oren, M. Malladi, M. Petriccione, K.C.De Braganca, M. Donzelli, C. Fischer, S. Vitolano, G.P. Wright, L. Ganshaw, M. Marrano, A. Ahmed, J. DeStefano, E. Danzer, M.H.A. Roehrl, N.J. Lacayo, T.C. Vincent, M. R. Weiser, M.S. Brady, P.A. Meyers, L.H. Wexler, S.R. Ambati, A.J. Chou, E. K. Slotkin, S. Modak, S.S. Roberts, E.M. Basu, D. Diolaiti, B.A. Krantz, F. Cardoso, A.L. Simpson, M. Berger, C.M. Rudin, D.M. Simeone, M. Jain, C.M. Ghajar, S. K. Batra, B.Z. Stanger, J. Bui, K.A. Brown, V.K. Rajasekhar, J.H. Healey, M. de Sousa, K. Kramer, S. Sheth, J. Baisch, V. Pascual, T.E. Heaton, M.P.La Quaglia, D. J. Pisapia, R. Schwartz, H. Zhang, Y. Liu, A. Shukla, L. Blavier, Y.A. DeClerck, M. LaBarge, M.J. Bissell, T.C. Caffrey, P.M. Grandgenett, M.A. Hollingsworth, J. Bromberg, B. Costa-Silva, H. Peinado, Y. Kang, B.A. Garcia, E.M. O'Reilly, D. Kelsen, T.M. Trippett, D.R. Jones, I.R. Matei, W.R. Jarnagin, D. Lyden, Extracellular vesicle and particle biomarkers define multiple human cancers, Cell 182 (2020), 1044.e18.
[15] J. Huan, Y. Gao, J. Xu, W. Sheng, W. Zhu, S. Zhang, J. Cao, J. Ji, L. Zhang, Y. Tian, Overexpression of CD9 correlates with tumor stage and lymph node metastasis in esophageal squamous cell carcinoma, Int. J. Clin. Exp. Pathol. 8 (2015) 3054.
[16] Y. Murayama, Y. Shinomura, K. Oritani, J. Miyagawa, H. Yoshida, M. Nishida, F. Katsube, M. Shiraga, T. Miyazaki, T. Nakamoto, S. Tsutsui, S. Tamura, S. Higashiyama, I. Shimomura, N. Hayashi, The tetraspanin CD9 modulates epidermal growth factor receptor signaling in cancer cells, J. Cell. Physiol. 216 (2008) 135.
[17] H.X. Wang, C. Sharma, K. Knoblich, S.R. Granter, M.E. Hemler, EWI-2 negatively regulates TGF-β signaling leading to altered melanoma growth and metastasis, Cell Res. 25 (2015) 370.
[18] J.R. Hwang, K. Jo, Y. Lee, B.J. Sung, Y.W. Park, J.H. Lee, Upregulation of CD9 in ovarian cancer is related to the induction of TNF-α gene expression and constitutive NF-κB activation, Carcinogenesis 33 (2012) 77.
[19] S.E. Emam, H. Ando, A.S.A. Lila, T. Shimizu, K. Okuhira, Y. Ishima, M.A. Mahdy, F. S. Ghazy, I. Sagawa, T. Ishida, Liposome co-incubation with cancer cells secreted exosomes (extracellular vesicles) with different proteins expressions and different uptake pathways, Sci. Rep. 8 (2018) 14493.
[20] R. Reyes, B. Cardeñes, Y. Machado-Pineda, C. Cabañas, Tetraspanin CD9: a key regulator of cell adhesion in the immune system, Front. Immunol. 9 (2018) 863.
[21] M. Hemler, Targeting of tetraspanin proteins — potential benefits and strategies, Nat. Rev. Drug Discov. 7 (2008) 747.
[22] D. Liu, P. Guo, C. McCarthy, B. Wang, Y. Tao, D. Auguste, Peptide density targets and impedes triple negative breast cancer metastasis, Nat. Commun. 9 (2018) 2612.
[23] T. Suwatthanarak, M. Tanaka, T. Minamide, A.J. Harvie, A. Tamang, K. Critchley, S.D. Evans, M. Okochi, Screening and characterisation of CdTe/CdS quantum dot-binding peptides for material surface functionalisation, RSC Adv. 10 (2020) 8218.
[24] T. Suwatthanarak, I.A. Thiodorus, M. Tanaka, T. Shimada, D. Takeshita, T. Yasui, Y. Baba, M. Okochi, Microfluidic-based capture and release of cancer-derived exosomes via peptide–nanowire hybrid interface, Lab Chip 21 (2021) 597.
[25] T. Suwatthanarak, M. Tanaka, Y. Miyamoto, K. Miyado, M. Okochi, Inhibition of cancer-cell migration by tetraspanin CD9-binding peptide, Chem. Commun. 57 (2021) 4906.
[26] M. Zuidscherwoude, F. Göttfert, V.M. Dunlock, C.G. Figdor, G. van den Bogaart, A. B. van Spriel, The tetraspanin web revisited by super-resolution microscopy, Sci. Rep. 5 (2015) 12201.
[27] J. Fan, G.Z. Zhu, R.M. Niles, Expression and function of CD9 in melanoma cells, Mol. Carcinog. 49 (2010) 85.
[28] C. Espenel, E. Margeat, P. Dosset, C. Arduise, C. Le Grimellec, C.A. Royer, C. Boucheix, E. Rubinstein, P.-E. Milhiet, Single-molecule analysis of CD9 dynamics and partitioning reveals multiple modes of interaction in the tetraspanin web, J. Cell Biol. 182 (2008) 765.
[29] S. van Deventer, A.B. Arp, A.B. van Spriel, Dynamic plasma membrane organization: a complex symphony, Trends Cell Biol. 31 (2021) 119.
[30] T. Shoham, R. Rajapaksa, C.-C. Kuo, J. Haimovich, S. Levy, Building of the tetraspanin web: distinct structural domains of CD81 function in different cellular compartments, Mol. Cell. Biol. 26 (2006) 1373.
[31] D.R. Bond, R. Kahl, J.S. Brzozowski, H. Jankowski, C. Naudin, M. Pariyar, K. A. Avery-Kiejda, C.J. Scarlett, C. Boucheix, W.J. Muller, L.K. Ashman, M.J. Cairns, S. Roselli, J. Weidenhofer, Tetraspanin CD9 is regulated by miR-518f-5p and functions in breast cell migration and in vivo tumor growth, Cancers 12 (2020) 795.
[32] C. Xing, W. Xu, Y. Shi, B. Zhou, D. Wu, B. Liang, Y. Zhou, S. Gao, J. Feng, CD9 knockdown suppresses cell proliferation, adhesion, migration and invasion, while promoting apoptosis and the efficacy of chemotherapeutic drugs and imatinib in Ph+ ALL SUP-B15 cells, Mol. Med. Rep. 22 (2020) 2791.
[33] A. Hoshino, B. Costa-Silva, T.L. Shen, G. Rodrigues, A. Hashimoto, M. Tesic Mark, H. Molina, S. Kohsaka, A. Di Giannatale, S. Ceder, S. Singh, C. Williams, N. Soplop, K. Uryu, L. Pharmer, T. King, L. Bojmar, A.E. Davies, Y. Ararso, T. Zhang, H. Zhang, J. Hernandez, J.M. Weiss, V.D. Dumont-Cole, K. Kramer, L.H. Wexler, A. Narendran, G.K. Schwartz, J.H. Healey, P. Sandstrom, K.J. Labori, E.H. Kure, P. M. Grandgenett, M.A. Hollingsworth, M. de Sousa, S. Kaur, M. Jain, K. Mallya, S. K. Batra, W.R. Jarnagin, M.S. Brady, O. Fodstad, V. Muller, K. Pantel, A.J. Minn, M. J. Bissell, B.A. Garcia, Y. Kang, V.K. Rajasekhar, C.M. Ghajar, I. Matei, H. Peinado, J. Bromberg, D. Lyden, Tumour exosome integrins determine organotropic metastasis, Nature 527 (2015) 329.
[34] L.A. Hapach, J.A. Mosier, W. Wang, C.A. Reinhart-King, Engineered models to parse apart the metastatic cascade, npj Precis. Oncol. 3 (2019) 20.
[35] F. Martin, D.M. Roth, D.A. Jans, C.W. Pouton, L.J. Partridge, P.N. Monk, G. W. Moseley, Tetraspanins in viral infections: a fundamental role in viral biology? J. Virol. 79 (2005) 10839.
[36] P.A. Lazo, Functional implications of tetraspanin proteins in cancer biology, Cancer Sci. 98 (2007) 1666.

[37] C. Shu, S. Han, C. Hu, C. Chen, B. Qu, J. He, S. Dong, P. Xu, Integrin β1 regulates proliferation, apoptosis, and migration of trophoblasts through activation of phosphoinositide 3 kinase/protein kinase B signalling, J. Obstet. Gynaecol. Res. 47 (2021) 2406.
[38] M.A. Breau, A. Dahmani, F. Broders-Bondon, J.P. Thiery, S. Dufour, β1 integrins are required for the invasion of the caecum and proximal hindgut by enteric neural crest cells, Development 136 (2009) 2791.
[39] J. Song, J. Zhang, J. Wang, J. Wang, X. Guo, W. Dong, β1 integrin mediates colorectal cancer cell proliferation and migration through regulation of the Hedgehog pathway, Tumor Biol. 2015 (2013) 36.
[40] M.F. Santos, G. Rappa, J. Karbanová, C. Vanier, C. Morimoto, D. Corbeil, A. Lorico, Anti-human CD9 antibody fab fragment impairs the internalization of extracellular vesicles and the nuclear transfer of their cargo proteins, J. Cell. Mol. Med. 23 (2019) 4408.
[41] S. Buratta, B. Tancini, K. Sagini, F. Delo, E. Chiaradia, L. Urbanelli, C. Emiliani, Lysosomal exocytosis, exosome release and secretory autophagy: the autophagic- and endo-lysosomal systems go extracellular, Int. J. Mol. Sci. 21 (2020) 2576.
[42] P. Fuentes, M. Sesé, P.J. Guijarro, M. Emperador, S. Sánchez-Redondo, H. Peinado, S. Hümmer, S. Ramón, Y. Cajal, ITGB3-mediated uptake of small extracellular vesicles facilitates intercellular communication in breast cancer cells, Nat. Commun. 11 (2020) 4261.
[43] Z.W. Liu, Y.M. Zhang, L.Y. Zhang, T. Zhou, Y.Y. Li, G.C. Zhou, Z.M. Miao, M. Shang, J.P. He, N. Ding, Y.Q. Liu, Duality of interactions between TGF-β and TNF-α during tumor formation, Front. Immunol. 12 (2022), 810286.
[44] P. Hoppenz, S. Els-Heindl, A.G. Beck-Sickinger, Peptide-drug conjugates and their targets in advanced cancer therapies, Front. Chem. 8 (2020) 571.
[45] B. Paul, R.H. Gaonkar, D. Dutta, R. Dasi, B. Mukherjee, S. Ganguly, S.K. Das, Inhibitory potential of iRGD peptide-conjugated garcinol-loaded biodegradable nanoparticles in rat colorectal carcinoma, Biomater.Adv. 134 (2022), 112714.
[46] K. Ovejero-Paredes, D. Díaz-García, I. Mena-Palomo, M. Marciello, L. Lozano-Chamizo, Y.L. Morato, S. Prashar, S. Gómez-Ruiz, M. Filice, Synthesis of a theranostic platform based on fibrous silica nanoparticles for the enhanced treatment of triple-negative breast cancer promoted by a combination of chemotherapeutic agents, Biomater.Adv. 137 (2022), 212823.